The Meteorological Magazine

Me… …scale m…
Radar stu… …ll in Com…

… Vol. 11… …414

The Meteorological Magazine

May 1990
Vol. 119 No. 1414

551.509.313:551.509.5(41)

The Meteorological Office mesoscale model

B.W. Golding
Meteorological Office, Bracknell

Summary

A description is given of the Meteorological Office's mesoscale (15 km grid-spacing) forecasting model. Results of verification of model (objective) forecasts against human (subjective) forecasts for a selection of weather elements are given.

1. Introduction

Numerical weather prediction models in current operational use give valuable guidance to forecasters on the broad-scale atmospheric structure. In the Meteorological Office a grid-length of about 150 km is used in a global prediction model and half that in a regional model covering the North Atlantic and Europe. However, even this latter model cannot represent the topographic differences between parts of the United Kingdom which are important for short-period forecasting. A mesoscale numerical forecast model with very fine resolution has been developed to tackle this problem with the aim of providing guidance to forecasters on the local variations of weather in the period up to a day ahead. This model is closely tied to the regional model through its boundary conditions so it must be seen as a sophisticated tool for adding detail to the predictions of the coarser models. In particular it will not be able to correct timing errors in systems that pass through the boundaries. On the other hand, in slow moving situations the topographically induced effects should be well forecast and should be of considerable help to the local forecaster. It is widely recognized that model predictions of mesoscale systems that are not forced by topography will be difficult. However, the errors will often be in timing or location so that the products may still provide useful guidance on many occasions. It may also be that much of the mesoscale variation in weather from larger-scale systems is actually induced by topographic variations, perhaps through the surface temperature or moisture. In these cases the added detail will be of considerable value provided that the regional model has correctly predicted the large-scale evolution. Any anticipated errors in the large-scale timing or development will have to be taken into account when interpreting the mesoscale guidance. The remaining sections will describe the model formulation, the methods currently used for preparing the initial data, and some recent results. The model formulation is described more fully in Golding (1989).

2. The forecast model as at January 1990

2.1 Spatial resolution and coverage

The model presently has a 15 km grid-length and covers the British Isles and near Continent except for Shetland (see Fig. 1). With this resolution a reasonably faithful representation of the orography can be given, and the coastline, indicated by the zero height contour in Fig. 1, has a realistic shape. Nevertheless, individual peaks and valleys less than 30 km across cannot be represented. Their effects must be added to the model guidance by forecasters familiar with the small-scale climatology of each district.

2.2 Dynamics

The basic dynamical equations used by the model have been described for a dry atmosphere in Tapp and White (1976) and Carpenter (1979). The vertical

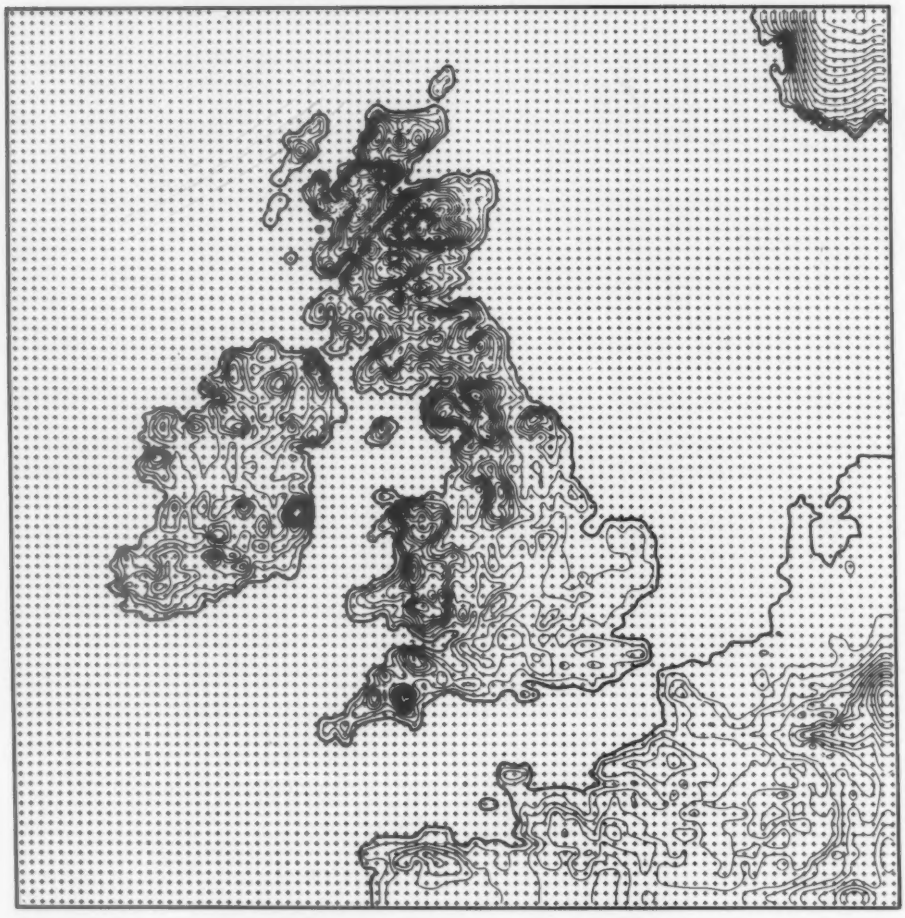

Figure 1. Model domain and orography. The grid points have a 15 km spacing and the contour interval is 50 m. The bold contour is at zero height and indicates the model coastline.

coordinate is height above the land surface. Thus, model surfaces follow the orography as shown in Fig. 2 for the current version with 16 levels. The lowest level is at 10 m and the spacing increases linearly from 110 m to 1510 m at the top. The highest level is at 12 010 m which is normally in the stratosphere. This arrangement gives five levels in the lowest kilometre and an almost constant spacing of 60 mb from there up to the tropopause.

The model is non-hydrostatic and compressible and so has prognostic equations for the vertical velocity and Exner pressure variable $\pi = (p/p_0)^{R/c_p}$ where R is the universal gas constant, c_p the specific heat at constant pressure and p_0 a reference pressure. It uses thermodynamic variables which are conserved in the processes of condensation and evaporation. The potential temperature and Exner variable are split into a basic state and deviation. Source terms represent contributions from the sub-grid-scale parametrizations for deep convection, radiation, precipitation and diffusion. The method of solution is a semi-implicit one in which the terms supporting sound waves in the basic state are separated and solved implicitly.

2.3 Radiation

The short-wave radiation budget is computed at two levels, the ground, and the highest cloud top if below 5 km. The transmission is obtained by applying, multiplicatively, transmission coefficients for Rayleigh scattering, water vapour absorption, aerosol scattering and cloud. Each is a function of bulk atmospheric quantities. The expression for cloud transmission was fitted to computations obtained using the model of Slingo and Shrecker (1982). At cloud top, absorption is parameterized as a function of solar zenith angle only, and is constrained not to exceed the long-wave cooling in the same layer.

The long-wave scheme uses a modified form of the scheme developed by Roach and Slingo (1979). The upward and downward fluxes of radiation are computed

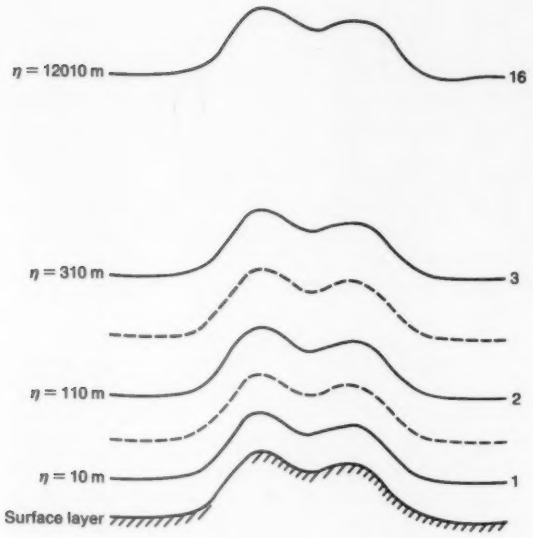

Figure 2. Vertical structure of the model. The vertical coordinate is height above ground (η) and there are 16 levels from 10 to 12 010 m. Wind pressure, temperature, humidity and cloud are specified at the main levels indicated by solid lines. Vertical velocity and turbulent kinetic energy are specified at intermediate levels (dashed lines).

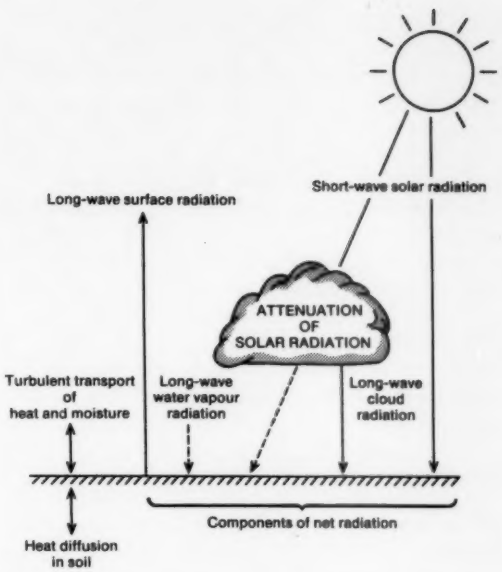

Figure 3. Schematic diagram of the processes involved in the surface heat balance of the model.

for each model level in five wavelength bands. The transmission functions are represented as products of functions for water vapour, carbon dioxide and cloud, the latter being weighted linearly by the maximum cloud fraction in the slab.

2.4 Surface exchanges

The surface heat balance consists of four components; the net radiation, the ground heat flux and the atmospheric sensible and latent heat fluxes (Fig. 3). The net radiation consists of the net long-wave flux, described in section 2.3, and the absorbed part of the solar radiation. The short-wave albedo is set to 0.18 over land surfaces except where snow is present.

The ground heat flux is obtained from the diffusion equation applied to the layer represented by the surface temperature T_* and the soil temperature T_s. The fluxes of heat, moisture and momentum into the atmosphere are computed using drag-law expressions with transfer coefficients computed from Monin–Obukhov similarity theory as a function of roughness length and Richardson number. Over Britain, roughness lengths were obtained from the drag-coefficient map of Smith and Carson (1977). Other land areas use a roughness length of 10 cm. Over the sea the wind-speed dependent formula of Charnock (1955) is used. The roughness length for heat and moisture is one fifth that for momentum and is not permitted to exceed 0.1 m.

In the flux of moisture, the surface humidity is unknown so it is eliminated using the concept of a surface resistance to evaporation after Monteith (1964). The resistance is set to zero over the sea or when dew is being deposited, and to 500 s m^{-1} elsewhere at night. Otherwise the resistance is computed from weekly estimates of soil moisture deficit extracted from the MORECS system (Thompson *et al.* 1981). Where moisture or snow is lying on the surface, a value of 50 s m^{-1} is used.

In order to avoid instability in the surface temperature T_*, the surface heat equation is integrated implicitly using the first term of a Taylor series expansion as an estimate of the sensitivity of each of the fluxes to variations in T_*.

2.5 Turbulent mixing

Vertical mixing is parametrized using a 1½-order closure scheme based on Yamada and Mellor (1979) as adapted by Smith (1984a, 1984b). In this scheme a formal expansion of the equations in mean and turbulent quantities is truncated after the second order. In the resulting set of equations, only the time rate of change (E) of turbulent kinetic energy (TKE) is retained, the equations for the other second-order quantities being reduced to diagnostic relations. The equation for E then contains four terms, representing generation of turbulence by shear, changes due to buoyancy (including latent heat release), turbulent transport of TKE and dissipation.

Manipulation of the second-order equations leads to flux gradient relationships with the mixing coefficients given by complex expressions involving E, buoyancy, shear and a diagnosed mixing length. The numerical solution for the turbulent fluxes is performed implicitly for all variables including the turbulent kinetic energy itself.

2.6 Grid-scale cloud and precipitation

In the advective and diffusive processes, the model uses variables which are conserved through changes of state. However, for the parametrization of radiation and precipitation, it is necessary to distinguish between vapour, water cloud, and ice cloud. Rain water is assumed to fall immediately and is not carried in the model. Snow is assumed to be indistinguishable from ice cloud. The diagnosis is performed using the mean and turbulent parts of the temperature and humidity distributions to define a probability distribution of unsaturated and saturated states within the grid volume. The distribution used has a top-hat shape. The proportion of saturated states is then the fractional cloud cover, and the excess water in them is the cloud water content.

The expression for the variance of the distribution contains two terms: the first represents turbulent variability while the second has been added to allow for non-turbulent variations which are assumed to become greater as the depth of the grid box increases. The phase of the cloud depends on whether the ambient temperature is above or below a critical temperature. The critical temperature is −15 °C unless snow is already present in which case it is 0 °C. The critical humidity for cloud formation is saturation over water unless snow is already present when it is saturation over ice. The effect of this formulation is shown in Fig. 4 where supercooled water cloud can deepen until it reaches the −15 °C level when it glaciates fully down to 0 °C.

The precipitation processes are modelled quite differently for ice cloud and liquid water cloud. Ice (or snow) is assumed to fall at a speed that is weakly dependent on mixing ratio (Heymsfield 1977) (approximately 1 m s^{-1} for dense cloud).

No snow will fall out of a cloudless layer with such a formulation so it effectively prevents snow falling through dry layers. In order to avoid this when high vertical resolution is used, a realistic evaporation is calculated over the depth of the layer and this overrides the calculation of fall-out from a layer when this would be smaller.

Below the freezing level, snow falls to the ground within a timestep. Both evaporation and melting are based on Rutledge and Hobbs (1983). Melting is computed as a function of precipitation rate and wet-bulb temperature.

Rain is formed from liquid water cloud by two processes, local production, and accretion on rain falling through the layer (Fig. 5). At the surface, the precipitation is defined as snow if the majority is snow or if the snow rate is greater than 0.2 mm h^{-1} (water equivalent).

2.7 Deep convection

The deep convection scheme was based originally on that of Fritsch and Chappell (1980). It retains their concept of diagnosing instability and then assuming that the resulting convection will last for many model timesteps. In the scheme here, convection lasts for one hour and is advected across the grid with the ambient wind at the middle level. Instability is diagnosed by lifting model layers to the next layer, where grid-scale vertical motion is upward, and then testing whether they are upwardly buoyant. If so, the parcel is lifted, with entrainment, until it is no longer buoyant. The parcel is detrained at this level with a small value of supersaturation, and with the parcel horizontal velocity. The mass flux in the updraught is related to the depth of cloud.

Instability is tested every 15 minutes so it is possible to have up to four such clouds in a grid square at one time. Precipitation is computed from the parcel supersaturation when it reaches cloud top if the cloud-top temperature is colder than −5 °C. Some condensate is detrained into

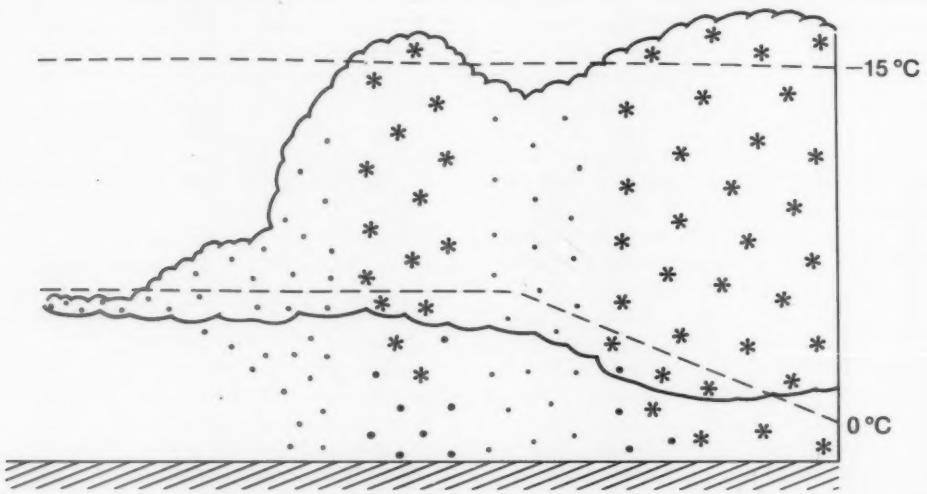

Figure 4. Schematic diagram of the representation of snow and rain in the precipitation scheme.

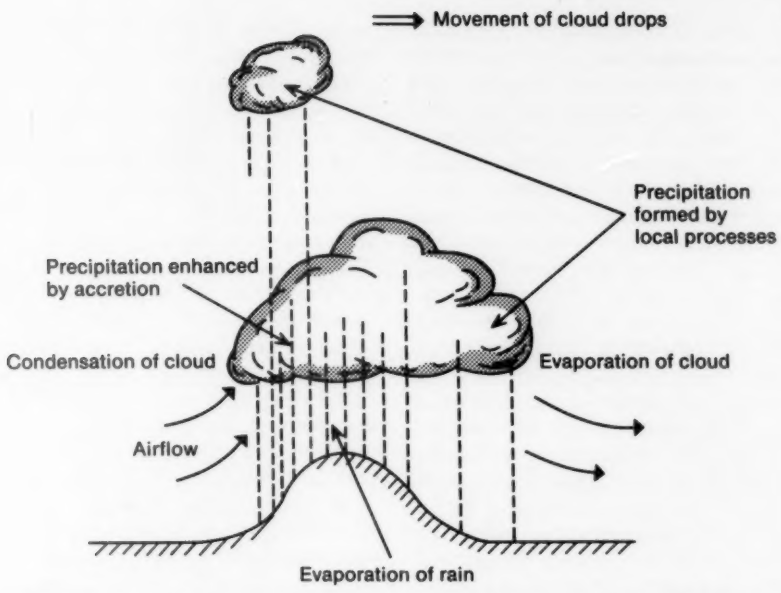

Figure 5. Schematic diagram of the processes involved in the liquid water precipitation scheme.

the anvil and some is evaporated in the downdraught to keep it saturated at cloud levels and 80% saturated below cloud. A cloud-top temperature-dependent efficiency factor is also applied, further reducing the precipitation from clouds with tops warmer than about −15 °C. In order to convert the precipitate into a rain rate it is necessary to diagnose a rain area. This is related to the depth of cloud and the shear between base and top. The downdraught mass flux is related to the mass of air lying beneath the cloud that is available for evaporative cooling, and to the rain rate.

If the temperature of the downdraught exceeds the ambient temperature at 10 m, it is assumed not to reach the ground and the effects of the outflow are ignored. At cloud base it has the ambient potential temperature and humidity and these are modified by evaporation as the air descends. The resulting modified air is detrained in the model's lowest layer.

The most important effect of the convection on the grid-scale flow occurs through the subsidence required to compensate for the convective-scale updraught and downdraught. This is modelled by a source term in the pressure equation. Since the model is non-hydrostatic, it responds with grid-scale vertical accelerations to redistribute the mass.

2.8 Aerosol

An estimate is made of the cloud condensation nucleus (CCN) concentration assuming no sources and sinks within the grid. A single concentration representative of the boundary layer is used and is advected with the 1010 m wind. Boundary values are fixed at 50 cm^{-1} on sea boundaries and 300 cm^{-1} on land boundaries. At present the CCN concentration does not influence the model evolution but is used in diagnosing visibility for output.

2.9 Boundary conditions

There are five boundaries to the mesoscale model, the four lateral boundaries and the top. Values from the fine-mesh model are used on each of them. The upper boundary is also adjusted so as to give a mass flux which compensates for any drift in the mean pressure at 5 km away from that prescribed from the fine-mesh model. The fine-mesh values are extracted at 3-hour intervals, interpolated in time and space and adjusted for the different orography. Pressures are recomputed from the interpolated surface pressure and potential temperature profile. Land surface and sea surface temperatures are interpolated separately.

3. Initialization

The representation of the initial state of the atmosphere is of critical importance to the quality of forecast that can be expected from the model. As with large-scale models, the constraints of near-geostrophy must be satisfied if a stable forecast evolution is to be obtained. However, a short-range forecast model must also be correctly initialized with cloud if the temperature and precipitation are to be realistically forecast. Indeed, the atmosphere 'remembers' much of its initial state over a 12-hour period on many occasions and this contributes to the accuracy of subjective forecasts based on modified extrapolation procedures.

Three sources of data are currently used to initialize each forecast. They are an interpolation of the latest fine-mesh forecast, a 3-hour mesoscale forecast, and observations. A cycle of 3-hour forecasts is maintained

throughout the day permitting a continuous passing forward of mesoscale forecast data where observations are not available. The interpolation of fine-mesh model fields is an important part of the mix since it is by this means that information about the synoptic-scale structure is obtained. This is the only way that upper-air observations reach the analysis as their resolution is too low to justify the effort of incorporating them directly on to the 15 km grid. The resolution of local-area TIROS operational vertical sounder retrievals is much better than radiosondes, but these lack detail in the vertical structure. Interpolation of the fine-mesh fields is a complex process since the models use different map-projections and a different vertical coordinate as well as the mesoscale model having finer resolution. In addition the specification of orography is quite different. For these reasons, interpolated data are not normally used in the boundary layer. Here the latest mesoscale forecast is used if available. It is also used as first guess for the moisture field and is filtered to give short-wavelength detail in all fields which is added to the smooth interpolated fields. This is justified on the assumption that such detail is often related to the detailed orography in the model. This combination of data from the two forecast models forms a 'hybrid' which is used as the first guess for the analysis procedure.

The initialization scheme can be run in two modes: interactive or objective. In the objective mode, the initialization uses surface reports of pressure, wind, rainfall, cloud cover, cloud base and 8-groups (cloud type/base groups), visibility, state of ground, snow depth, temperature and dew-point. These are obtained from reports in SYNOP, SHIP, LIGHT VESSEL, METAR, DRIBU, NCM and SREW codes. If a quality-controlled radar image and a calibrated Meteosat cloud-top temperature image are available for the analysis time, they will also be used. In the interactive mode, analysts can override either the observations or the analysis of any variable. They can also choose to use off-time images, a raw radar image or to recalibrate the Meteosat image. They can compare the vertical structure of the initialization against radiosonde ascents and modify accordingly. Finally, they have sferics reports available for guidance in the rainfall analysis.

Many of the observed variables are of little value in the model initialization in isolation. However, in combination with others, they are used to adjust other model fields in a consistent manner. This is particularly important for the humidity structure which has probably the most important control over mesoscale development.

The initialization procedure starts with the main dynamical fields of pressure, wind and potential temperature. First, the surface pressure is analysed from a first-guess interpolated fine-mesh field. This is followed by an analysis of wind components. Prior to this, however, the mesoscale forecast first guess is averaged with geostrophic winds based on the pressure analysis. This is particularly useful over the sea and where a sharp trough has been introduced in the pressure analysis. Following the wind analysis, pressure, wind and potential-temperature increments are computed for all levels from the adjustments made to the surface pressure and wind fields. The surface-wind adjustments are applied with decreasing weight up to 1010 m. The pressure adjustments are used to compute geostrophic wind and hydrostatic potential-temperature increments which are applied with decreasing weight up to 8010 m and shifted upstream with a 1:100 slope. The upstream direction is a mean for the whole domain. Below 1010 m the geostrophic wind adjustments have reduced weight.

The moisture distribution is then computed starting with an analysis of surface rainfall. Where available, this uses the radar image as first guess. Surface present weather and precipitation accumulations (SREWs) are used to estimate rates at observing stations. These are analysed assuming a small radius of influence within radar range, but a broader influence elsewhere. In the interactive mode, the analyst can use the satellite image and sferics reports to assist in finalizing this analysis. The overall cloud cover is analysed next. If available, the Meteosat cloud-top temperature image is used to compute a first guess assuming that all tops colder than 10 °C below predicted surface temperature must be cloud. After analysis of the surface reports, the satellite image is adjusted in areas of partial cloud to allow for the transmission of surface infra-red emission to the satellite. The adjusted image is then used to derive a cloud-top distribution (if an image is not available, the mesoscale-forecast cloud top is used). The forecast cloud base is then adjusted to ensure that it is at least 200 m below cloud top, and is then used as first guess for an analysis of cloud-base observations. If the cloud-base analysis conflicts with cloud top, one or the other is adjusted. Below 8000 ft (2438 m) the base is assumed correct and above 8000 ft the top is preferred. Using the analysed (and checked) cloud cover, base and top as constraints, a cloud-cover analysis is then performed for every model level. This is done by first interpreting the observed 8-groups in the light of the first guess interpolated to each observation position, to give a profile of cloud-cover values at model levels. These are then analysed a level at a time. At this point the analyst may select to view profiles of temperature and cloud fraction at several locations to ensure that they are realistic and consistent (e.g. boundary-layer cloud does not extend above the boundary-layer inversion). If locations are selected for which radiosonde ascents are available, these are displayed as a guide. Modification can be made to either or both profiles, and applied to an area delineated on the map by the analyst.

The final set of analyses relate to surface conditions. They are the visibility, surface wetness or snow depth (frozen deposits are treated as negative, liquid ones as positive with state of ground reports of dry, moist, flooded and frost interpreted quantitatively), surface

temperature and dew-point. The humidity mixing ratio is calculated at screen level and then assumed constant up to 20 m. This, together with the visibility analysis, is used to estimate a cloud condensation nucleus distribution for the boundary layer.

The humidity is set at each level to be consistent with the analysed cloud cover using a simplified form of the relation in the forecast model. The cloud liquid/ice mixing ratio is then initialized with empirical profiles for different analysed rain rates. These are then adjusted interactively to give the analysed rate when the model precipitation equations are applied. The surface temperature analysis is used to adjust soil temperatures. Then temperature profiles are adjusted from screen-level upwards to spread the influence of surface observations and to ensure that there is no convective instability except within analysed cloud where it must be consistent with the model turbulence equations. While this is done, the deviation of the mean temperature from that in the first guess is minimized so as to avoid unbalancing the model. Finally, the vertical velocities required to replace cloud which is precipitating are calculated and the divergence fields adjusted accordingly.

The impact of the interactive technique has been tested in several case-studies (Wright and Golding 1989) and has been found to be greatest when there is little large-scale control of the evolution. A notable example was a case from Project Haar (Findlater *et al.* 1989) in which the objective analysis misrepresented the coverage of fog over the North Sea. In the forecast this resulted in premature clearance of the fog (Fig. 6(a)). Interactive modification of the initial fog distribution produced a much improved forecast (Fig. 6(b)) in which the fog was retained over a much larger area (in reality it did not lift to stratus around the coast and did not penetrate so far in land).

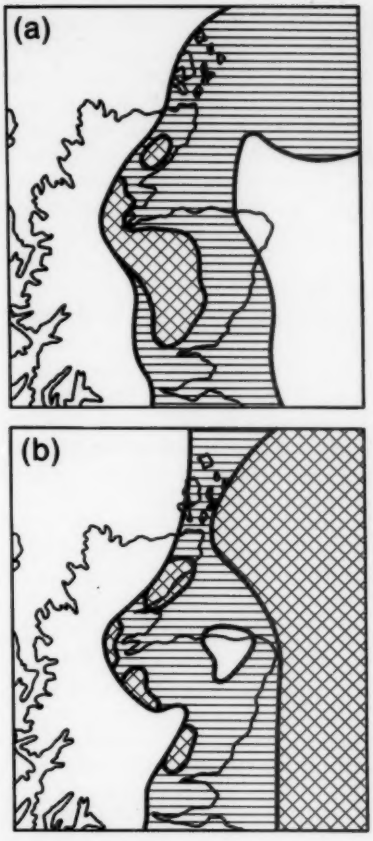

Figure 6. Nine-hour forecasts from 06 UTC on 29 April 1984 in a fog situation. (a) Initial conditions from the objective analysis, and (b) initial conditions modified via interactive VDU taking account of satellite imagery. Low cloud is shown by horizontal shading, and fog by hatching.

4. The operational trial

4.1 General aspects

A weekly trial of the forecast system in the first part of 1984 was followed by an operational trial from October 1984–January 1985 in which a single 12-hour forecast was run each day from 06 UTC. The results were sufficiently encouraging for a second extended trial to be started in April 1985. Meanwhile, the efficiency of the forecast was improved so that it now takes about 1 minute per hour of forecast time. Major improvements have been: the turbulence scheme using conservative variables in June 1985; the revised ice-phase precipitation scheme in September 1985; the system for carrying information forward from one forecast to the next in November 1985; the cloud-top radiation budget in May 1986 and the snowmelt formulation in December 1986. Since March 1987 a range of products has been disseminated by digital facsimile to a small number of local forecast stations for assessment there. During August 1988 the Central Forecasting Office (CFO) began routine use of the interactive mesoscale initialization scheme to introduce radar and satellite imagery into the forecasts. In October 1989 the model domain was enlarged to include the North Sea, the multi-level long-wave radiation scheme was incorporated, and the cloud-top temperature dependence of shower precipitation was introduced.

The objective assessment of this trial has been carried out at all observing stations for most observed variables and permits great flexibility in the comparisons that can be made. It has been supplemented by various subjective assessment techniques including comparison with the local area forecast for Bracknell, with temperatures forecast by Weather Centres for gas boards, and with cloud and visibility predictions at the local stations receiving model products.

In general, the synoptic-scale evolution predicted by the mesoscale model differs little from the fine-mesh model — as intended. It does not generally improve on timing and development errors and does not consistently forecast mesoscale dynamical developments such as rain

bands with accuracy. One difference that has been noted is a tendency to speed up cold fronts — thus exacerbating a tendency for the fine-mesh model to be too fast in this respect. At its present stage of development it should therefore be seen as a detailed diagnostic tool which enables the effects of topographic variation to be taken into account and, by using more sophisticated physical parametrizations, enables the variables required by forecast users to be predicted directly.

A general assessment of the usefulness of the forecasts can be obtained by analysing references to the products in the Synoptic Reviews (SRs) issued by CFO. Due to time of availability, comments appear in Part 2 or 3 of the review and frequently are used to support forecasts already disseminated in Part 1. References are also made to advise those stations receiving mesoscale products of aspects to be disregarded, and to advise other stations of useful features of the forecast. In Table I references are analysed into three categories for each weather element. The first category contains references where CFO are communicating useful model guidance. The second contains references to features which are considered unlikely but that should be noted for caution. The third category is of features to be ignored. The period of analysis is October–November 1989 during which 73 forecasts were referenced.

Consistent with subjective impressions the wind is very reliable, but it is not often an important element in central guidance. The temperature is referred to most often, usually in comparison with Model Output Statistics (MOS) hence the large number of entries in the caution column. Precipitation is most often referred to in support of an enlargement of a fine-mesh rain area or to introduce an area of showers missed by the fine mesh. Cloud and fog are recognized to be unreliable. However, in the anticyclonic spell in November 1989, both were referenced repeatedly.

Table I. Analysis of model references in synoptic reviews, October–November 1989

Element	Number of references		
	Guidance	Caution	Ignore
Cloud	19	3	5
Temperature	32	15	2
Wind	10	1	0
Precipitation	12	2	4
Fog	11	7	3

4.2 Specific aspects

4.2.1 Temperature

With the first model level at 10 m, screen-level temperature has to be diagnosed from the predicted ground- and first-level values. At present a linear interpolation in height is used when an inversion is present and the average of the two taken otherwise. This procedure produces good results provided the cloud is reasonably correct. Errors in cloud have most effect at night in winter and in the day in summer. Fig. 7 shows percentages of maximum and minimum temperature forecasts within given tolerances of observations for each month since autumn 1985. All observing stations in the British Isles are included. The results depend on the weather type: mild, cloudy weather producing better statistics than clear weather in both summer and winter.

November and December statistics indicate that the warm bias in night-time temperatures had been removed in the latest version of the model. In November, the 12 UTC run had a mean error between ±0.2 °C at all forecast times. The 00 UTC run had an increasing negative error reaching −0.6 °C by dawn which corrected itself after sunrise. This was much smaller in December and was probably related to the cloud deficit in the early part of the forecast (see below). Also in November, taking minimum temperatures for 18–06 UTC, air frost occurred in 14.7% of observations and was forecast in 15.8% with a hit rate of 70% and a false-alarm rate of 35%.

The geographical distribution of large errors in January 1989 is shown in Figs 8(a) and 8(b) showing that many of the errors in Fig. 7 are occurring at highland or coastal locations, unrepresentative of the surrounding area.

The mesoscale model predictions are significantly better than those obtained directly from the fine-mesh model. By statistically relating fine-mesh predictions to observations at 32 specific sites, MOS predictions score about 5% more cases within 2 °C than the mesoscale model. The model, however, does better in unseasonable weather.

A comparison with subjective forecasts issued to the gas boards is shown in Table II. The predictions are from 15-hour forecasts of the model. The subjective forecasts are issued at 1530 LST for 3 a.m. but rather earlier for 3 p.m. giving the model a slight advantage in the latter prediction. The results are similar at most locations but reflect the difficulty of interpolating between land and sea points at Cardiff and possibly Southampton, and the effect of the urban setting of London Weather Centre.

4.2.2 Wind

Wind speed and direction predictions are generally considered to be good although light winds tend to be overpredicted. In November 1989, observed winds below 6 kn were predicted with a significant positive mean error of about 3 kn, an r.m.s. error of 4–5 kn and r.m.s. direction errors of 40–50°. Observed winds of 6–16 kn had a zero mean error, an r.m.s. error of 4 kn and r.m.s. direction errors of about 30°. Observed winds of 16–27 kn had a small negative mean error, an r.m.s. error of 6 kn and r.m.s. direction errors of 20–25°. Above this speed, the sample is small and is dominated

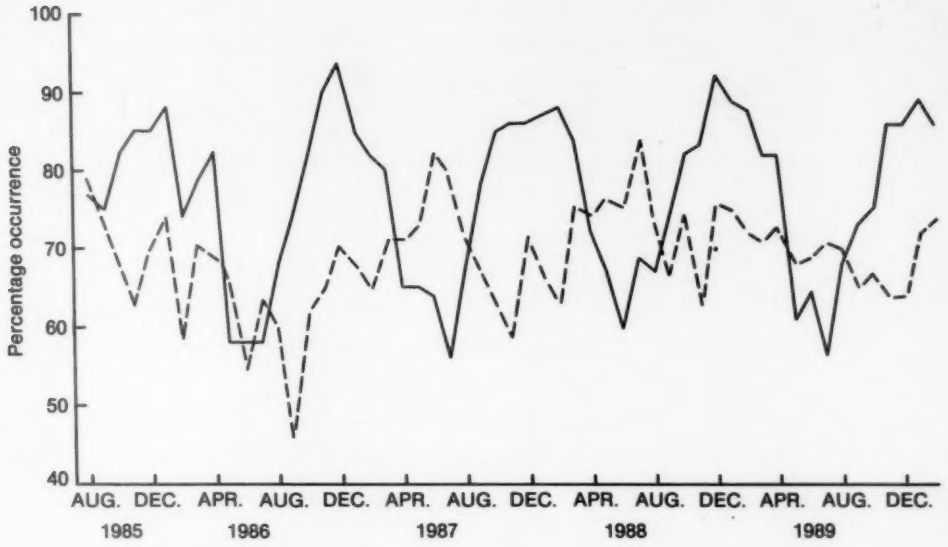

Figure 7. Percentages of predicted maximum (continuous line) and minimum (dashed line) temperatures within 2 °C of observed values for a sample of stations in the British Isles for 1985–90.

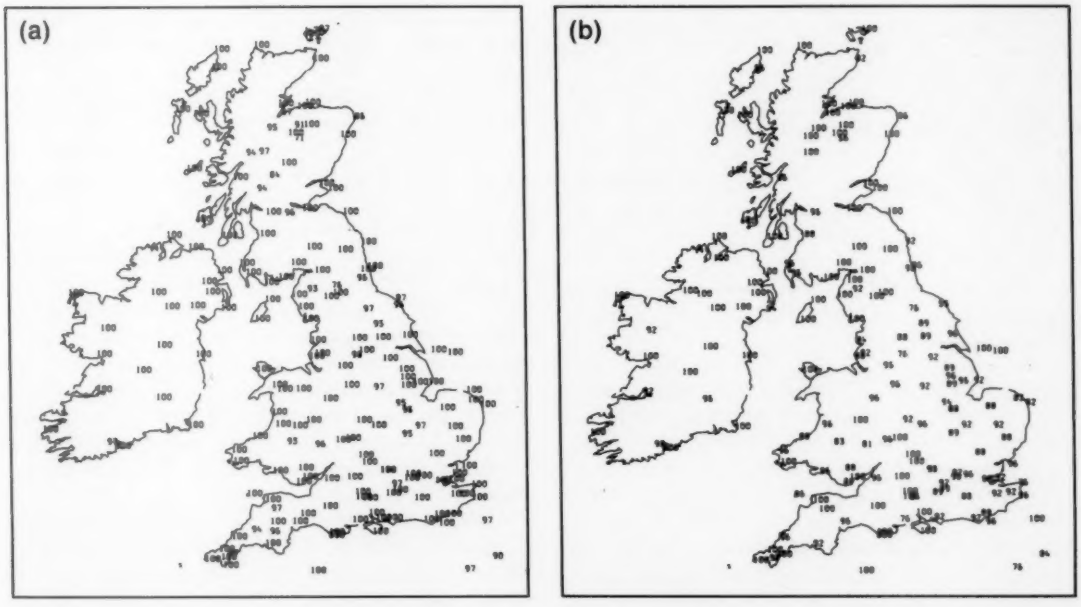

Figure 8. Maps of percentages of forecast screen temperatures within 4 °C of observed values in January 1989. (a) 15-hour forecasts for 15 UTC, and (b) 18-hour forecasts for 06 UTC.

by unrepresentative locations such as Cairn Gorm and Great Dun Fell. At all observed speeds, the statistics are affected by large positive speed errors at some inland stations in the Republic of Ireland and at some valley locations in Scotland; and large negative speed errors at Cairn Gorm, Great Dun Fell and Cape Wrath. The geographical distribution of errors in January 1989 is shown in Fig. 9. Most inland stations have an r.m.s. vector error of less than 5 kn. The fine-mesh forecasts, adjusted for altitude, show worse direction errors at low speeds, and worse speed errors at high speeds.

Comparisons of model with subjective forecasts have been carried out at Manchester and Glasgow for 9-hour forecasts. The forecasters extracted model predictions from charts and recorded their own predictions based on terminal aerodrome forecasts (TAFs) for their own

Table II. Percentage of subjective and mesoscale forecasts of 03/15 UTC temperature within 2° of observed in 1989

Station	03 UTC		15 UTC	
	Forecaster	Mesoscale	Forecaster	Mesoscale
Glasgow	73	83	80	79
London	88	75	79	85
Southampton	83	86	83	81
Cardiff	84	76	87	82
Nottingham	—	—	81	81

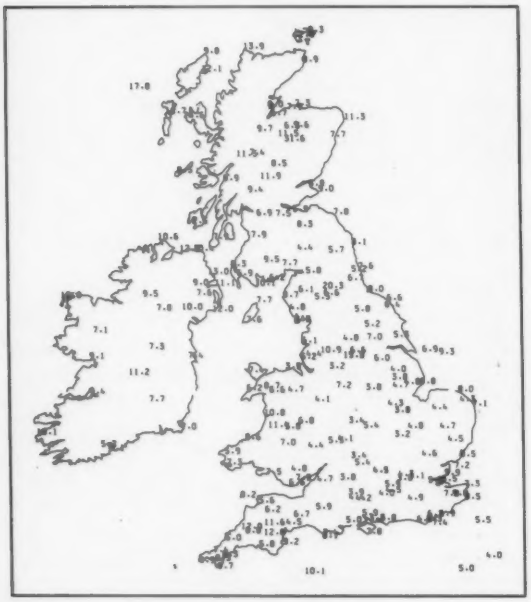

Figure 9. Map of root-mean-square vector wind errors (kn) in 15-hour predictions for 15 UTC in January 1989.

and a remote airport. Cases with observed wind speed below 5 kn were omitted from the direction comparison. The results are shown in Table III.

An example of a wind forecast is shown in Fig. 10. The observations are for 15 UTC on 25 January 1990 at the height of a storm which caused extensive damage. At this time the area of strongest winds covered much of south and central England and was characterized by inland wind speeds of about 40 kn. Exposed locations, particularly on Salisbury Plain and near the coast were experiencing 50 kn. The forecast was initialized at midnight and successfully predicted the general level of the strong winds, though not the more extreme observations. Note the reduced strength (35 kn) in much of the Home Counties as a result of the higher roughness lengths used in the model there.

4.2.3 Cloud

Since the latest version of the model was introduced in October 1989, there has been a marked reduction in cloud after initialization which gradually recovers over 6–9 hours. The reason for this is not yet known. The underprediction is particularly noticeable below 2000 ft (610 m).

Cloud is characterized by both cover and height in the observations, so it is difficult to devise a verification scheme which adequately measures the overall skill. For this reason, the accuracy of predicting a series of user-related thresholds is tested. For instance, one series of tests measures the skill in predicting 3 oktas or more of cloud with a base below 1000 ft (305 m), 2000 ft (610 m) or 6000 ft (1829 m). For each test, four measures of skill are tabulated — the frequency with which it was forecast (which may be compared with the actual frequency); the percentage of actual occurrences that were correctly forecast (the hit rate); the percentage of forecasts of the event which were wrong (the false-alarm rate), and the Hansen and Kuiper skill score, defined as the percentage of occurrences correctly forecast less the percentage of non-occurrences wrongly forecast.

In November 1989 there were 3 oktas or more of cloud with a base below 6000 ft (1829 m) in about 60% of observations. In general, the model forecasts achieved a 60–70% hit rate and 20–30% false-alarm rate. About

Table III. Assessment of model/forecaster predictions of wind for 09/21 UTC in 1989

Station	Speed errors (kn)		Direction errors (deg)	
	Mean	r.m.s.	Mean	r.m.s.
Glasgow	0.3/1.0	4.1/3.9	10/0	36/31
Aberdeen	2.2/1.3	4.6/4.4	5/1	30/33
Manchester	0.1/0.7	3.3/3.7	7/5	29/27
Blackpool	1.2/0.7	4.4/3.6	6/5	31/32

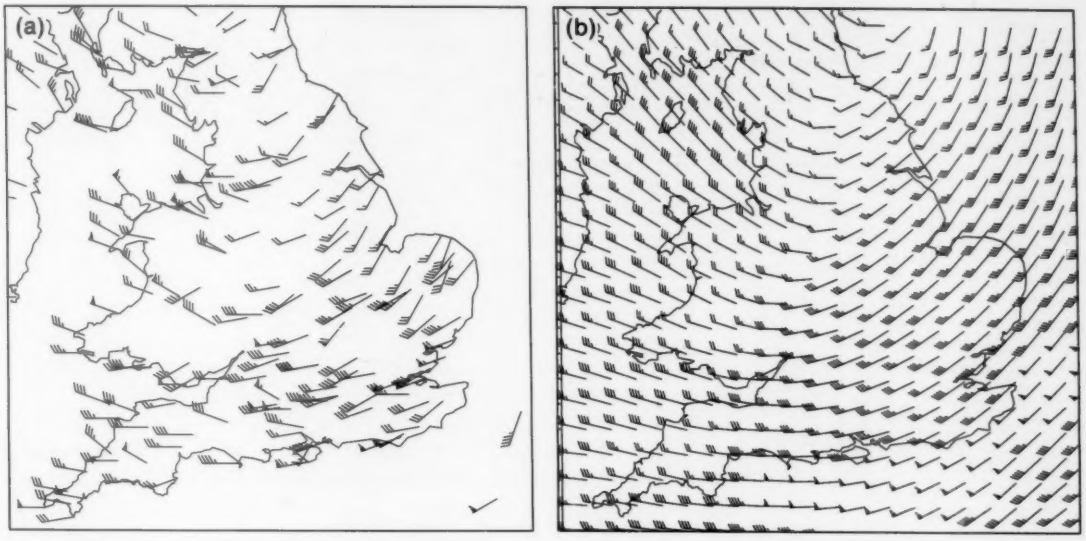

Figure 10. Mean winds (conventional symbols) at 15 UTC on 25 January 1990. (a) Observed, and (b) 15-hour forecast.

45% of observations met a 5 oktas threshold. For these the model achieved the same hit rate with a false-alarm rate of 30–40%. For lower height-thresholds, the hit rate reduced and the false-alarm rate increased. The statistics are very variable geographically and are not obviously related to topography.

Table IV shows comparative results for model/forecaster predictions of significant cloud below 1000 ft at several stations during 1989. The forecasters extracted the model predictions from charts and recorded their own forecasts based on TAFs, local area forecasts, etc. Note the geographical bias in the stations represented here.

The potential usefulness of the model in forecasting cloud base can be gauged from the comparisons with observations in Fig. 11. They show the evolution of the cloud base at Leuchars through the period 24–27 May 1987. To facilitate comparison, the observations have been moved to the nearest model level and these have been plotted at a nearby representative height (i.e. 500, 1000, 2000, 3000 ft). Apart from the forecast from 12 UTC on 24 January which lowered the base too early, they would all have given useful guidance to a forecaster.

An example of a forecast of cloud distribution is shown in Fig. 12. During early January 1987, the British Isles were affected by an extremely cold air mass which formed over the USSR and moved westwards across Europe. The cold air with temperatures below −20 °C over Europe developed convective cloud as it moved over the warmer sea (temperature 8–10 °C) which led to heavy snowfall over windward coasts. The cloud pattern is well picked out in the infra-red image (Fig. 12(a)) from the NOAA-9 satellite on the morning of the 12th. In particular the cloud crosses the Lizard and Land's End peninsulas in Cornwall and considerable snow was

Table IV. Skill scores for 3 oktas or more cloud below 1000 ft in 1989 — model/forecaster. See text for definition of terms.

Station	Times assessed (UTC)	Occasions observed	Occasions forecast	Hit rate	False-alarm rate	Skill score
Glasgow	09/21	43	39/45	35/51	62/51	30/47
Aberdeen	09/21	57	48/74	40/63	52/51	35/55
Manchester	09/21	36	34/51	31/58	68/59	26/52
Blackpool	09/21	54	21/59	9/48	76/56	6/41
Lyneham	09/12/15	148	82/164	28/64	49/42	23/55
Brize Norton	09/12/15	127	74/118	31/53	46/43	27/46
Wattisham	09/15	23	10/28	30/78	30/36	29/73
Marham	09/15	41	39/48	46/66	51/44	40/59
Honington	09/15	71	33/82	30/68	36/41	27/60
Coningsby	09/15	56	30/56	23/46	57/54	20/41

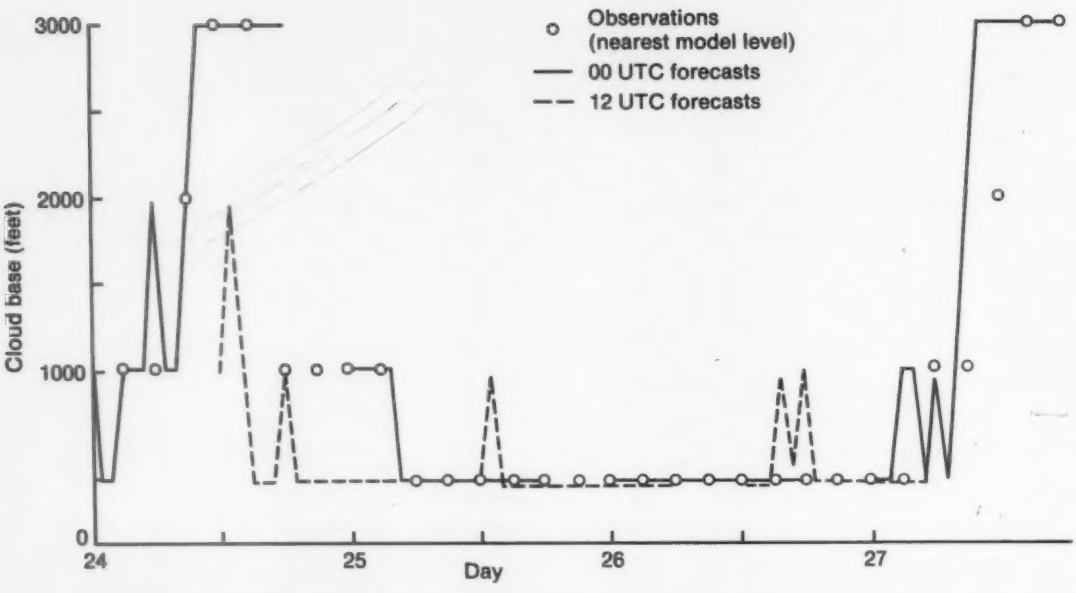

Figure 11. Forecast cloud base at Leuchars from T+1 to T+18 for 24–27 January 1987, compared with observations.

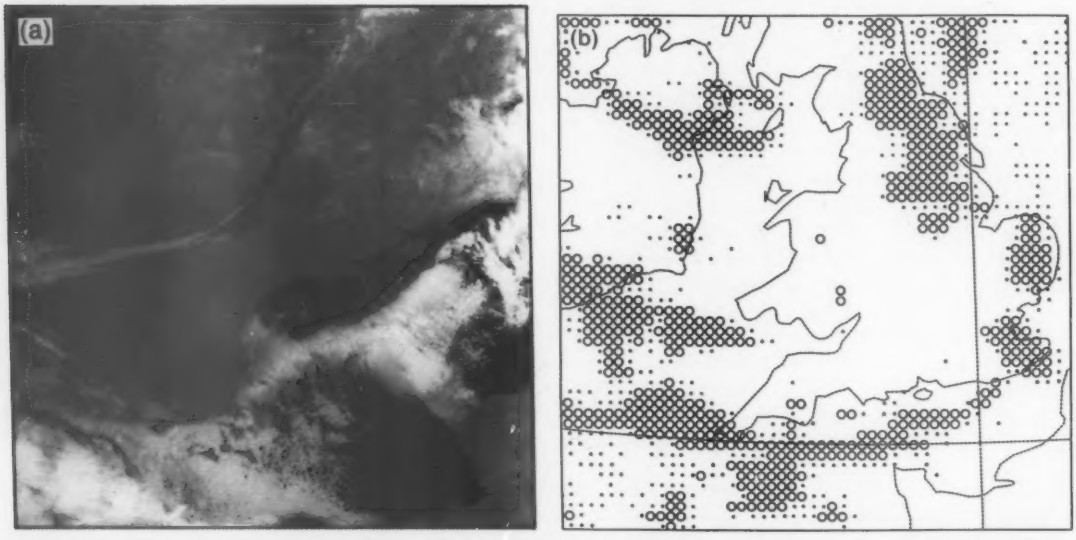

Figure 12. Cloud distribution at about 03 UTC for 12 January 1987. (a) NOAA-9 infra-red image at 0410 UTC, and (b) 9-hour forecast of total cloud cover. In (b) dots represent 4–7.5 oktas and open circles represent 7.5–8 oktas.

deposited in this area. The model's 9-hour low-cloud prediction (Fig. 12(b)) accurately portrays this cloud distribution and realistic snow amounts were forecast.

4.2.4 Visibility

In diagnosing visibility from model results, it is recognized that it may fall substantially before the humidity reaches saturation, even locally. Thus the criterion for cloud formation can be used for fog but not for mist or haze. It is also recognized that the relationship between visibility and water content depends on the cleanliness of the air. The visibility is therefore calculated from three quantities; the 10 m relative humidity and liquid water content, and the boundary-layer CCN concentration.

By its nature, fog is a local phenomenon often developing in hollows and along water courses at a scale of 1 km or less. Such patchiness is clearly impossible to predict with a 15 km resolution model. Although generally unreliable, model forecasts have provided useful guidance on several occasions when other techniques were uncertain. When using the results, it

must always be remembered that the model cannot, at present, distinguish between shallow fog, deep fog and stratus below 200 ft, and is attempting to give a forecast representative of a 15 km square.

Statistics for November 1989 show that the performance of the 00 UTC forecast was far better than that from 12 UTC. The 00 UTC forecast increased its fog coverage to about twice that observed by dawn and retained that level through the day for 200 m fog, but reduced it to the correct frequency for thinner fog and mist. The 12 UTC forecast cleared most of the observed fog very quickly and then gradually developed it again. By 06 UTC it had nearly four times the observed frequency of 200 m fog. For afternoon forecasts from the 00 UTC run, the hit rate was near 50% for the 200 m, 1 km, and 5 km thresholds. However, the false-alarm rate decreased from 75% for 200 m fog to below 50% for 5 km. The overprediction in the afternoon was due to too wide a distribution and fog was actually underpredicted in south-east England. Very few false alarms were forecast for this area. Details of the visibility prediction during 11–22 November 1989 are shown for Wattisham in Fig. 13. The overall trends are well captured by the model indicating that it is responding to forcing and initial conditions in a realistic manner. However, the forecasts show more variability than the observations, especially between fog and mist, suggesting that a more sophisticated parametrization of the growth of fog droplets may be needed.

Results from several airfield stations are shown in Table V for the accuracy of predictions of aviation fog during the day. The results are heavily weighted towards performance in the anticyclonic spell in November/December when the model predictions scored more hits

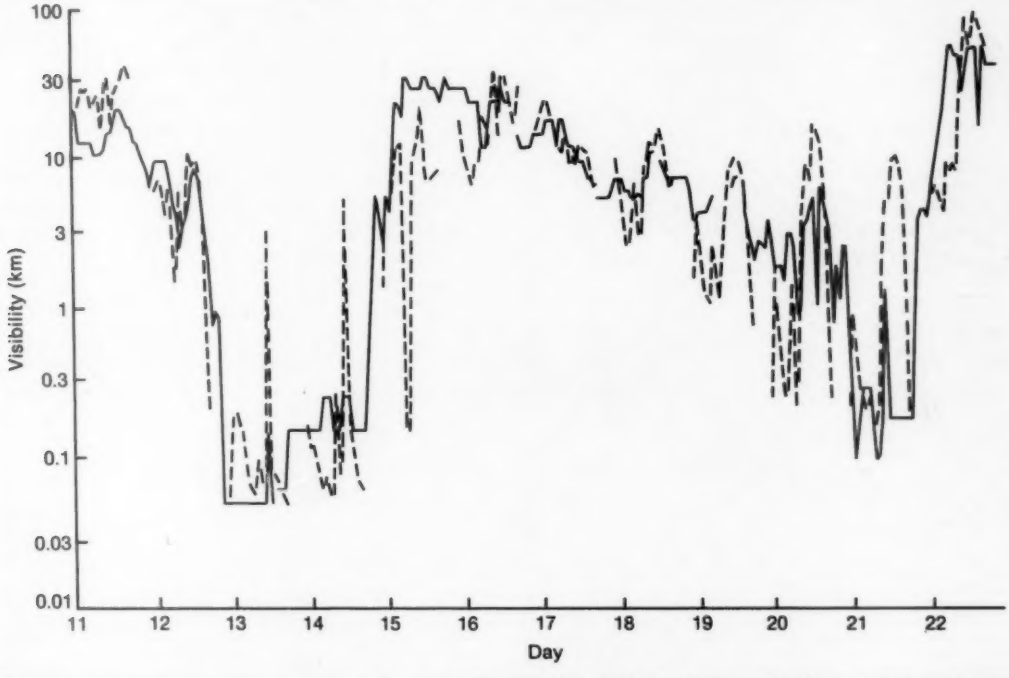

Figure 13. Observations (continuous line) and forecasts from 00 UTC (dashed line) of visibility at Wattisham, 11–22 November 1989.

Table V. Skill scores (model/forecaster) for daytime visibility below 1 km in 1989. See text for definition of terms.

Station	Times assessed (UTC)	Occasions observed	Occasions forecast	Hit rate	False-alarm rate	Skill score
Lyneham	09/12/15	29	37/14	38/31	70/36	35/30
Brize Norton	09/12/15	16	45/12	75/56	73/25	71/56
Wattisham	09/15	10	13/4	70/40	54/0	67/40
Marham	09/15	13	20/11	54/46	65/45	50/45
Honington	09/15	19	34/12	58/47	68/25	53/47
Coningsby	09/15	16	33/13	50/63	76/23	45/62

than the forecaster at most stations, especially in the afternoon (15 UTC).

Fig. 14 shows an example of a fog forecast from July 1986. The difficulty of verification is well illustrated by the small number of stations which actually lie within the forecast fog area. The erroneous sea fog is due to saturation of cold air flowing off the land. The mechanism is similar to sea smoke but is occurring on too large a scale in the model.

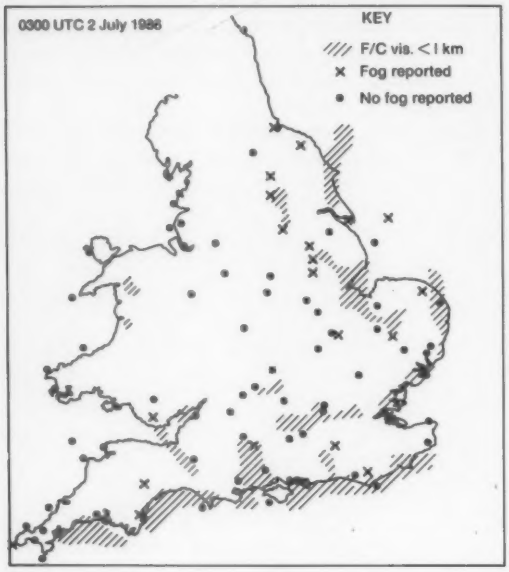

Figure 14. Comparison of observed fog areas 02–04 UTC with 9-hour forecast for 03 UTC on 2 July 1986.

4.2.5 Precipitation

The precipitation pattern usually follows that of the fine-mesh model, though with rather more light rain and showers. However, the finer resolution permits a better representation of orographic enhancement and rain shadow. A comparison between forecast 12-hour accumulations and observations for the month of January 1989 is shown in Figs 15(a) and 15(b). The general pattern is in good agreement, especially in Scotland where extremely large values were recorded. Fine-mesh model accumulations for the same period were less than half of the recorded totals.

The model's main deficiency is in the excessive prediction of small amounts of rain, especially as showers. The latter error is much improved since the introduction of the new version of the model. However, there is some evidence of an increase in the forecasting of spurious heavy showers. Results for December still indicate very light rain being predicted about twice as often as it occurs at night with a much smaller overprediction in the day. The fine-mesh model predicts about half as much very light rain as occurs in the day and 70–75% at night. However, for moderate and heavier rain both models overpredict at night and underpredict during the day.

During the period of snow threat in December 1989, the performance of the mesoscale model was generally encouraging and its usefulness was referred to in several SRs. The overall statistics, however, show about ten

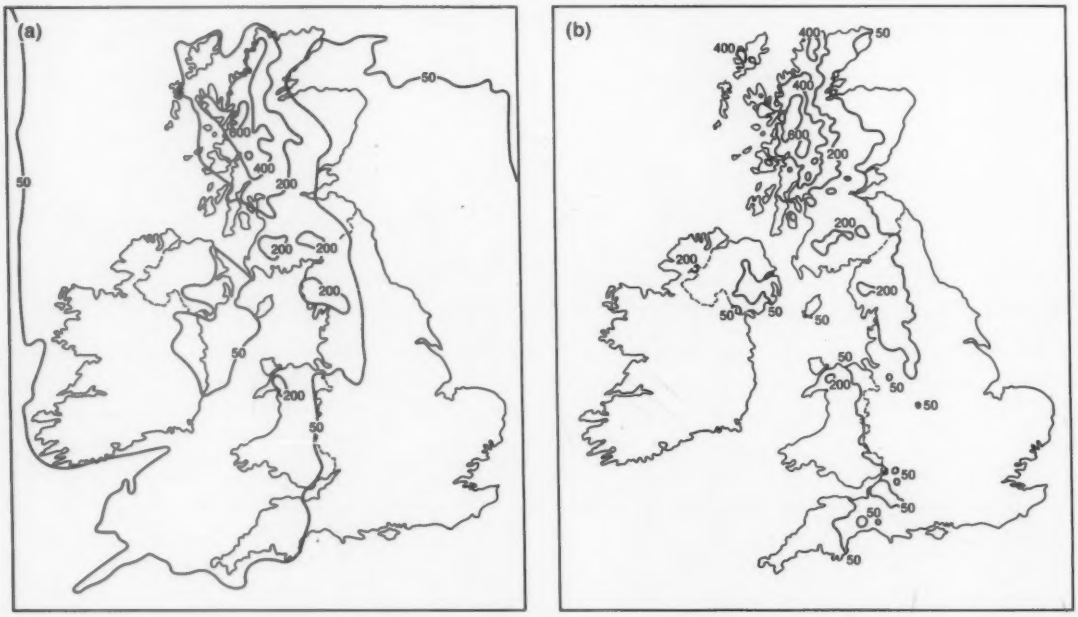

Figure 15. Rainfall totals (mm) for January 1989. (a) Sum of totals from the first 12 hours of each forecast, and (b) actual totals from the climatological rain-gauge network.

times as many occasions of snow predicted as observed and hit rates mostly in the range 20–40%. Applying the criterion to fine-mesh data that snow will occur if the freezing level is below 1000 ft gave prediction rates much closer to reality but a zero hit rate.

Forecasts of precipitation distribution are difficult to verify in a way that reflects their usefulness, especially in showery situations. A successful forecast of showers is therefore presented to illustrate the model's potential. On 24 May 1989 extensive thunderstorms affected much of England. The radar network recorded the development as shown in Fig. 16. At 11 UTC the area of rain in the Midlands remained from a mesoscale convective system (MCS) which moved north from France (Fig. 16(a)). This was not captured by the model (Fig. 16(c)). However, the new development to the south-west of London was well predicted in both time and location (Fig. 16(d)). The predicted showers over London were a little premature, and those over Wales and the north-west rather too extensive. As the afternoon progressed, the new showers spread towards London and south-west along a convergence line; and then also extended north-west from London, linking with the MCS in the north Midlands. This was well predicted by the model, though perhaps with the rain spreading rather too far east by this time.

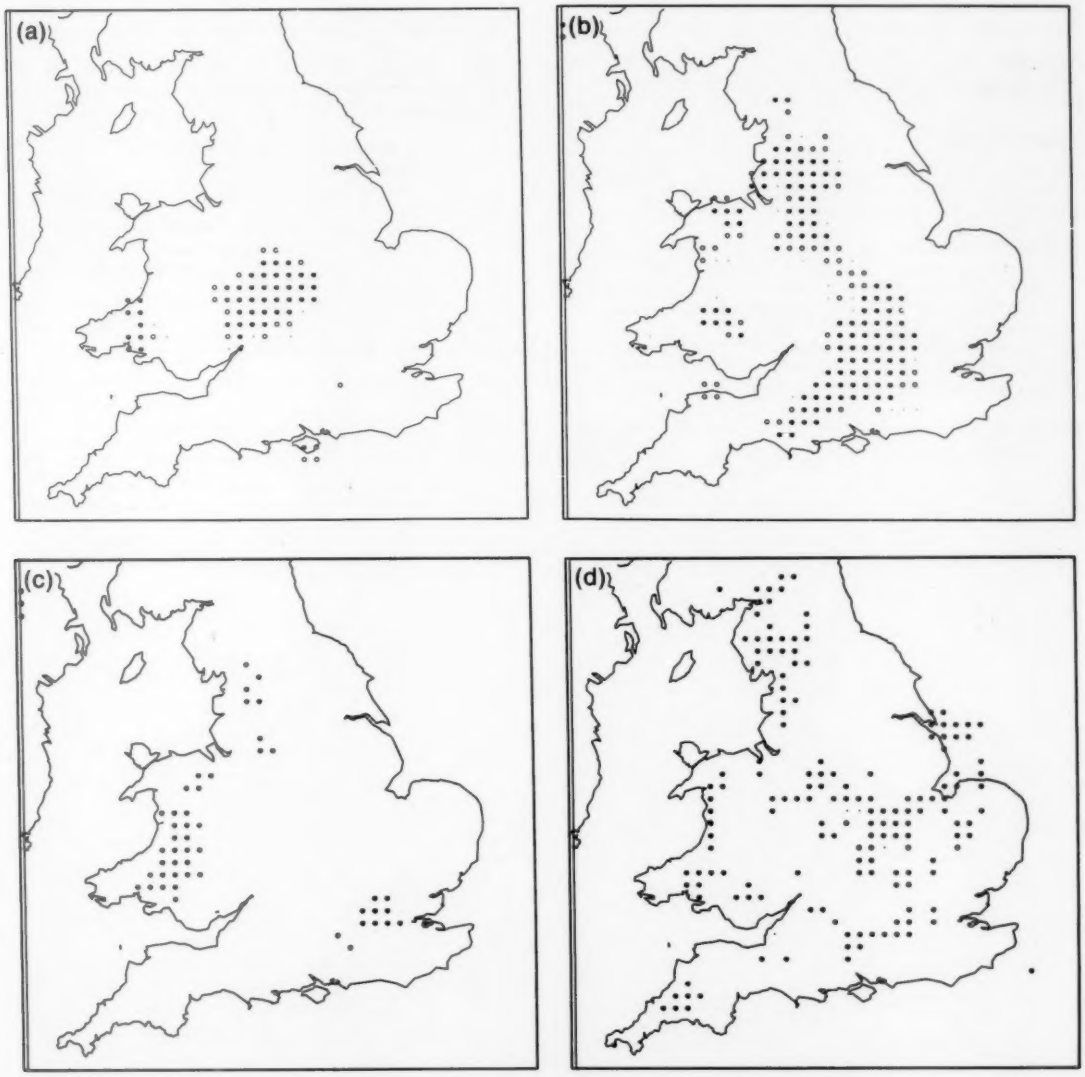

Figure 16. Distribution and development of showers and thunderstorms on 24 May 1989. (a) Radar observation at 11 UTC when the first showers developed south-west of London, (b) radar observation at 15 UTC, (c) 11-hour forecast for 11 UTC, and (d) 15-hour forecast for 15 UTC. Rainfall intensities are shown (in ascending order) by small dots, open circles and large dots.

5. Future Developments

Later this year, the mesoscale model will be transferred to the new Cray YMP supercomputer along with the operational forecast suite. The increased power will be used to increase the number of levels to meet requirements for low-cloud precision and to raise the top of the model to 15 km. A multi-level short-wave radiation scheme will also be implemented. Later, an improved advection scheme will be implemented, allowing a lower level of computational diffusion, which should also benefit the cloud forecasts. Improvements in data will come primarily from increased use of products from AUTOSAT-2, the Meteorological Office's satellite imagery processor. Dissemination of products will be improved by running the mesoscale forecast before the fine mesh, and by extensions to the GRAFNET facsimile network, resulting in quicker and more widespread availability of the model products.

References

Carpenter, K.M., 1979: An experimental forecast using a non-hydrostatic mesoscale model. *Q J R Meteorol Soc*, **105**, 629–655.

Charnock, H., 1955: Wind stress on a water surface. *Q J R Meteorol Soc*, **81**, 639–640.

Findlater, J., Roach, W.T. and McHugh, B.C., 1989: The haar of north-east Scotland. *Q J R Meteorol Soc*, **115**, 581–608.

Fritsch, J.M. and Chappell, C.F., 1980: Numerical prediction of convectively driven mesoscale pressure systems. Part I: Convective parameterization. *J Atmos Sci*, **37**, 1722–1733.

Golding, B.W., 1989: The Meteorological Office experimental mesoscale numerical weather prediction system: July 1989. (Unpublished, copy available in National Meteorological Library, Bracknell.)

Heymsfield, A.J., 1977: Precipitation development in stratiform ice clouds: a microphysical and dynamical study. *J Atmos Sci*, **34**, 367–381.

Monteith, J.L., 1964: Evaporation and environment. *Symp Soc Exp Biol*, **19**, 205–234.

Roach, W.T. and Slingo, A., 1979: A high resolution infrared radiative transfer scheme to study the interaction of radiation with cloud. *Q J R Meteorol Soc*, **105**, 603–614.

Rutledge, S.A. and Hobbs, P.V., 1983: The mesoscale and microscale structure and organization of clouds and precipitation in midlatitude cyclones. VIII: A model for the "seeder-feeder" process in warm frontal rainbands. *J Atmos Sci*, **40**, 1185–1206.

Slingo, A. and Schrecker, H.M., 1982: On the shortwave radiative properties of stratiform water clouds. *Q J R Meteorol Soc*, **108**, 407–426.

Smith, F.B. and Carson, D.J., 1977: Some thoughts on the specification of the boundary layer relevant to numerical modelling. *Boundary Layer Meteorol*, **12**, 307–330.

Smith, R.N.B., 1984a: The representation of boundary layer turbulence in the mesoscale model. Part I — The scheme without changes of state. (Unpublished, copy available in National Meteorological Library, Bracknell.)

—, 1984b: The representation of boundary layer turbulence in the mesoscale model. Part II — The scheme with changes of state. (Unpublished, copy available in National Meteorological Library, Bracknell.)

Tapp, M.C. and White, P.W., 1976: A non-hydrostatic mesoscale model. *Q J R Meteorol Soc*, **102**, 277–296.

Thompson, N., Barrie, I.A. and Ayles, M., 1981: The Meteorological Office Rainfall and Evaporation Calculation System MORECS (July 1981). *Hydrol Memo, Meteorol Off*, No. 45.

Wright, B.J. and Golding, B.W., 1989: The impact of the interactive mesoscale initialisation. (Unpublished, copy available in National Meteorological Library, Bracknell.)

Yamada, T. and Mellor, G.L., 1979: A numerical simulation of BOMEX data using a turbulence closure model coupled with ensemble cloud relations. *Q J R Meteorol Soc*, **105**, 915–944.

551.578.45:551.501.81:555.555.6(423)

Radar study of the snowfall in south-west Cornwall on 12 January 1987

W.S. Pike
19 Inholmes Common, Woodlands St. Mary, Newbury, Berkshire RG16 7SX

Summary

A heavy snowfall affecting south-west Cornwall during January 1987 is analysed using surface observations, Camborne 2 km radar data, and AVHRR satellite pictures to determine its causes, geographical extent and temporal limits.

1. Introduction

The general synoptic situation featuring extremely cold air advecting from the east during 12 January 1987 is shown in Fig. 1. Transfer westwards of convective cloud formed in cold air along a major convergence line over the relatively warm English Channel is shown in two AVHRR infra-red satellite pictures taken at 0410 and 0829 UTC on 12 January (Fig. 2). Note that the Lizard Peninsula is cloud-covered in the latter picture.

Lumb (1988) has described heavy snowfall affecting only the south-west of Cornwall, and an interesting report of 'pack snow' causing slight to moderate icing on the m.v. *Shell Explorer*, which was sailing through the snowfall in the English Channel off the Lizard that day, has been documented by Kain (1988) and Pike (1990a). It was deduced that these snowfalls had come within the 70 km range of Camborne's fine-mesh (i.e. 2 km × 2 km) radar coverage and that a study of radar images of precipitation at suitable intervals should be rewarding. These images are shown in Fig. 3 and are selected from a sequence originally recorded at 15-minute intervals.

2. Snowfall interpretation

Four Camborne hourly radar scans from 0300 to 0600 UTC on the 12th (Figs 3(a) to 3(d)) show bands of cold-frontal precipitation moving away south-westwards. Ignoring stationary ground-clutter returns from the hills around Camborne (Hensbarrow Down etc.) stippled areas represent slight snow (averaged over 2 km × 2 km squares) falling with equivalent rainfall rates of less than 0.5 mm hr^{-1}. Black areas represent areas of at least moderate snow with equivalent rainfall rates of 0.5 mm hr^{-1} or more. Isolated cells first appear east of the Lizard at 0600 UTC and thereafter continue to develop and move westwards at about 12–15 kn during

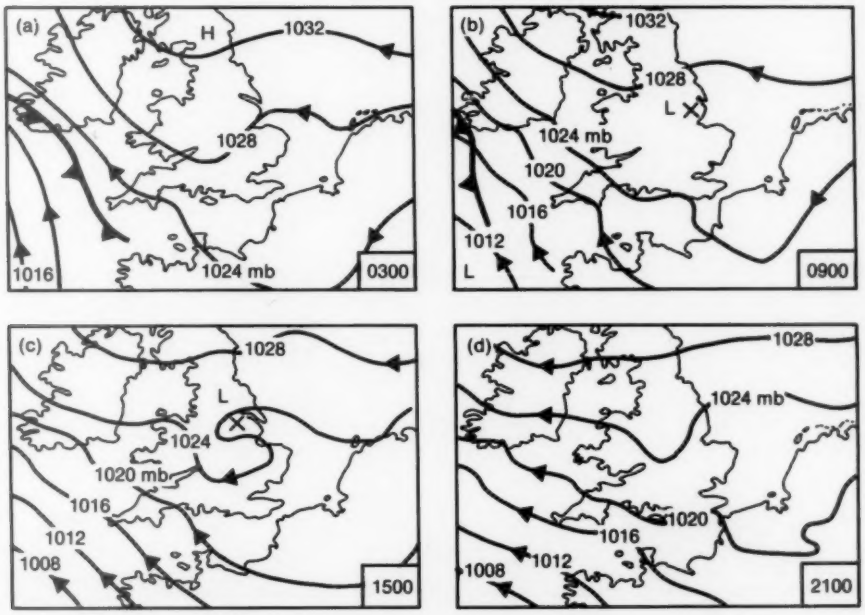

Figure 1. Surface synoptic charts for 0300, 0900, 1500 and 2100 UTC on 12 January 1987.

Photographs by courtesy of University of Dundee

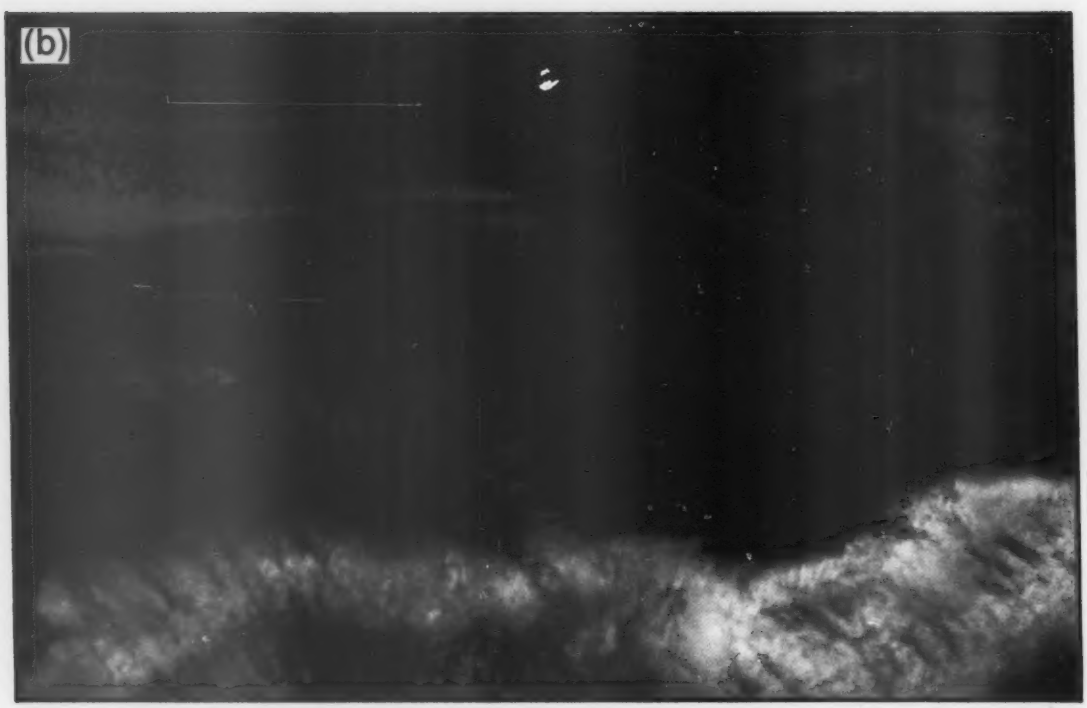

Figure 2. NOAA AVHRR infra-red satellite pictures for (a) 0410 UTC and (b) 0829 UTC on 12 January 1987.

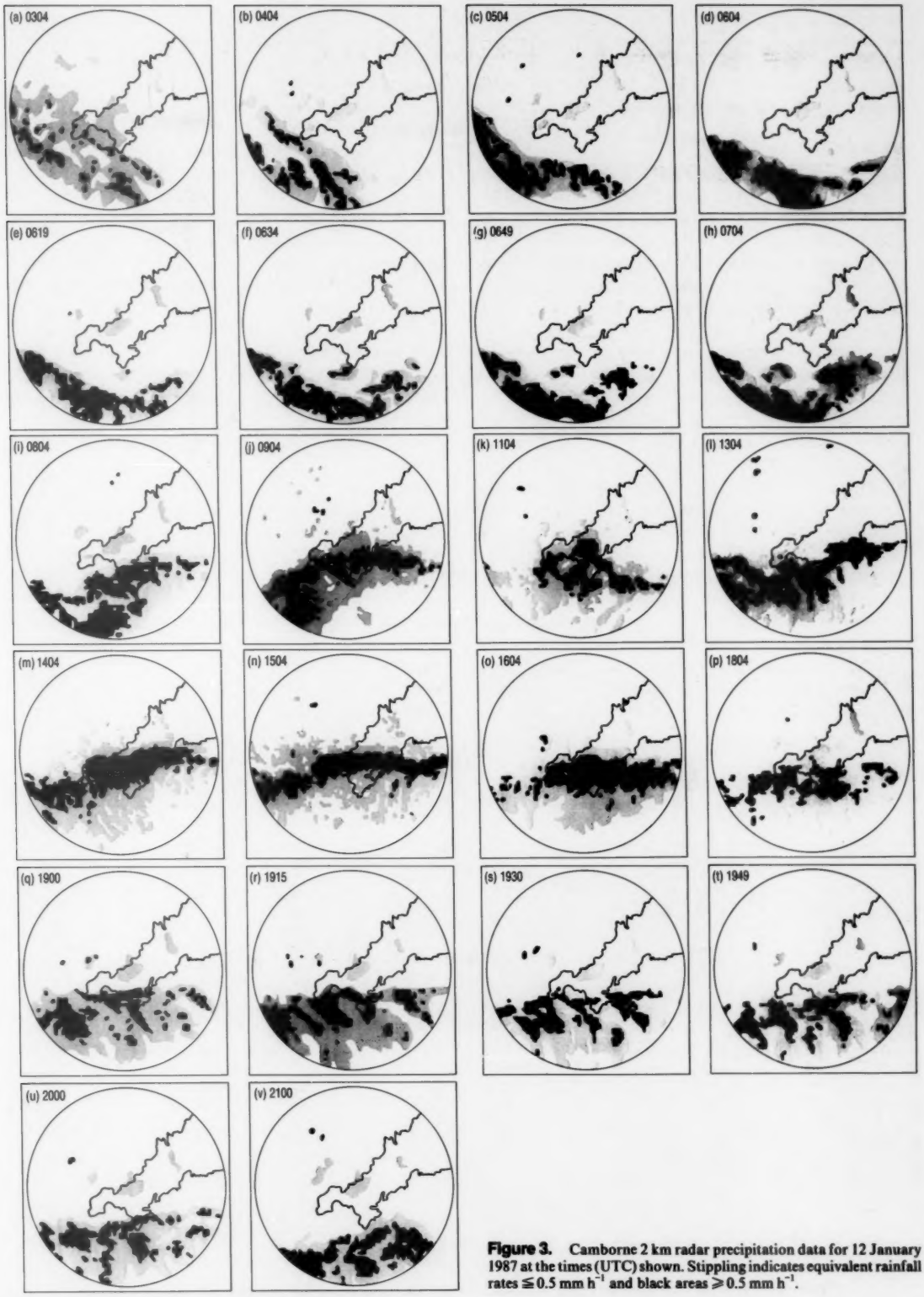

Figure 3. Camborne 2 km radar precipitation data for 12 January 1987 at the times (UTC) shown. Stippling indicates equivalent rainfall rates $\leqslant 0.5$ mm h^{-1} and black areas $\geqslant 0.5$ mm h^{-1}.

the next hour (Figs 3(e) to 3(h)). Further cells of precipitation merge together into a more or less continuous belt as they develop over the sea to the south-east, and snow begins to fall over the Lizard Peninsula between 0700 and 0800 UTC as this belt moves north-westwards. By 0900 UTC the snow belt covers much of south-west Cornwall, the precipitation zone never being more than 50 km wide, with the heavier snow area occupying up to half of this width. Fig. 2(b) for 0829 UTC gives the distinct impression that a series of convective cells were being built up primarily by the strong south-east to east-south-easterly over-water flow as it met lighter north-easterly to east-north-easterly low-level land-breezes along the length of a major convergence line which by now had propagated westwards along the English Channel from Sussex to west Cornwall.

As 'tracers' of the land-breeze, shallow 'plumes' of convective cloud are revealed by the NOAA AVHRR infra-red satellite pictures (Fig. 2) to be streaming downwind from promontories (especially The Needles on the Isle of Wight — see Fig. 2(a)) and also from the Wye Gorge, as a well-developed land-breeze drains down from the Forest of Dean over the warmer water of the Severn Estuary and the Bristol Channel.

East to west orientation of the precipitation belt axis appears to have closely correlated with a median position for the English Channel coastal convergence during this period (0900–2100 UTC on 12 January 1987), along or close to a line from Falmouth to Penzance at the boundary between the two (over land and over sea) low-level airflows.

Figs 3(j) to 3(n) show the behaviour and movement of the precipitation belt during daylight hours on the 12th. Probably the belt is genuinely narrow in the extreme south-east where cells are developing over the sea, but this might be due to a range- or masking-factor associated with the radar itself. A few breaks do appear at about 1100 UTC (Fig. 3(k)) but the precipitation remains continuous and more or less stationary during the day, although the heavier cells do tend to merge and the band moves a little further north during the afternoon. When breaks did appear in the morning, individual cells could be traced moving along the band through the pattern of general slight snow, as had been suspected earlier over the Thames Estuary (Pike 1990b) and after Passarelli and Braham (1981). The signature of land-breeze involvement may well be the sharp landward edge of precipitation (as in Fig. 3(l)) in comparison with the ragged seaward edge where irregular uplift is taking place.

The snow belt reaches its most northerly point over St. Austell Bay towards 1400 UTC (Fig. 3(m)), when perhaps the diurnal effects of land-breezes were weakest, before beginning to edge southward again. The 1504 UTC image introduces a narrow band of heavier snow 10–20 km wide, which is a feature of the following 3 hours as the belt continues to move southwards (Figs 3(n) to 3(p)) exhibiting a notably straight and sharp northern edge from 1800 to 2000 UTC indicating a strengthening land-breeze involvement. The black echelon-shaped precipitation areas appear to be a typical signature of convergent airflows being active in their formation. They move quite rapidly, at maybe

Figure 4. Car buried under extensive snow drift at RNAS Culdrose, near Helston, Cornwall on 12 January 1987.

25–35 kn, from east to west between 1900 and 2000 UTC and would seem to be particularly worthy of note. The snow finally clears the Lizard peninsula at around 2100 UTC having given substantial dry snowfall over the past 14 hours, there being a particularly sharp northern edge to the snow-affected areas.

Fig. 4 shows drifts to car-top height at the Royal Naval Air Station at Culdrose following snowfalls of 20–30 cm experienced during the 12th. On the Isles of Scilly, Tresco Botanical Gardens lost 70% of its trees and shrubs (many of which were subtropical species) during this brief period of extreme cold. Staff arrived on Monday 12 January in almost continuous heavy snow showers which left 9 inches (23 cm) lying by the end of the day when temperatures had fallen to −8.0 °C.

It should be noted that these heavy snowfalls in the south-west occurred immediately prior to record low 1000–500 mb thickness values arriving from the east. Readings of 500 dam at Larkhill (at 1200 UTC on the 12th) and 502 dam (at Camborne and Valentia by 0000 UTC on the 13th) appear to be the lowest values recorded there since regular upper-air soundings began over 50 years ago.

3. Conclusions

Fig. 5 demonstrates the close relationship between Camborne radar returns and the snow depths measured in south-west Cornwall on the 12th. When integrated over 6-hour periods (0900–1500 and 1500–2100 UTC) the Camborne 2 km data gives a very good indication of

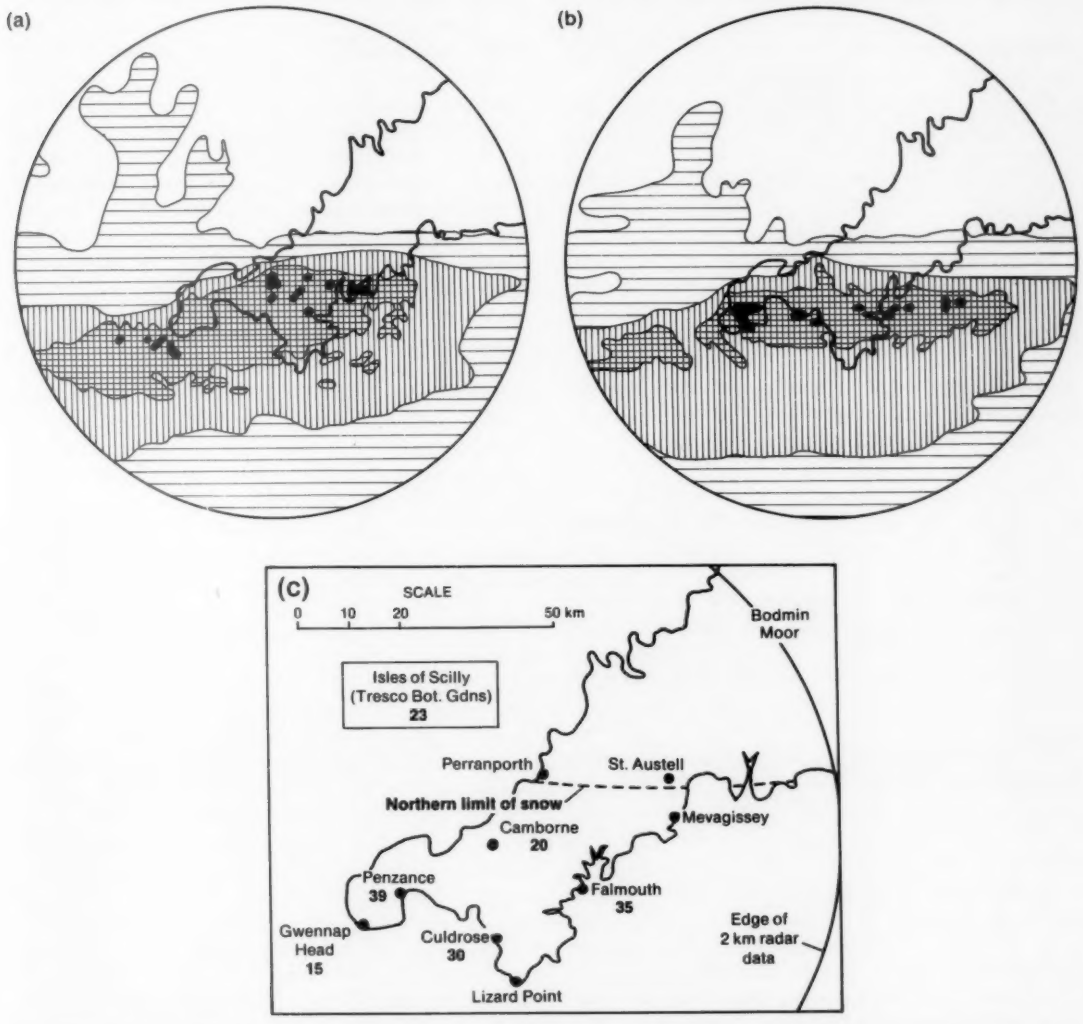

Figure 5. Integrated Camborne 2 km × 2 km radar precipitation data for the 6-hour periods (a) 0900–1500 UTC and (b) 1500–2100 UTC on 12 January 1987 related to (c) snowfall (cm) reported to have occurred during 12 January 1987. In (a) and (b) integrated rates of equivalent rainfall are indicated by horizontal shading (< 1.0 mm h^{-1}), vertical shading (1.0–2.9 mm h^{-1}), hatching (3.0–4.9 mm h^{-1}) and black (≥ 5.0 mm h^{-1}).

average snowfall intensity experienced over these particular time spans. The hatched areas clearly indicate those regions in which at least moderate snowfall predominated, taking the form of heaviest accumulations affecting a 25 km wide belt whose axis lay from approximately Falmouth (where 35 cm fell) to Penzance (39 cm).

Acknowledgements

To Meteorological Office staff at Bracknell, particularly to Geoff Monk of the Nowcasting and Satellite Applications Branch for supplying the Camborne 2 km radar data and integrations. Also to Commander P.L. Stubbs, RN, for kindly sending observations and photographs from RNAS Culdrose, and to J. Webb of 'TORRO' for additional snow depth observations.

References

Kain, D.G., 1988; Ice accretion; English Channel. *Mar Obs*, **58**, 13.

Lumb, F.E., 1988; Letter to *Weather*, **43**, 31.

Passarelli R.E. Jr. and Braham, R.R. Jr, 1981; The role of the winter land breeze in the formation of Great Lake snowstorms. *Bull Am Meteorol Soc*, **62**, 482–491.

Pike, W.S., 1990a; Land-breezes, snowfalls, and cold air convergence near coastlines in southern Britain. *Mar Obs*, **60**, 26–32.

—; 1990b; Persistent coastal convergence in a heavy snowfall event on the south-east coast of England. *Meteorol Mag*, **119**, 21–32.

Notes and news

Hydrologists meet to study precipitation measurement problems

(Note based on a news release from the WMO Press Office)

The summer of 1989 serves as a reminder that a deficiency of rainfall, especially like that over England and Wales, causes many hardships to the public and industry.

If anything, small rainfalls require more careful measurement than large ones if their benefits are to be maximized. But there is still a requirement for research into the attainable accuracy measurement of all rainfalls at points or their estimation over areas, both over land and sea.

The WMO has been involved in the study of methods of precipitation measurement for more than 30 years. With its Members, it has conducted many trials and tests of different instruments and methods in different parts of the world, but a number of problems remain.

The International Workshop on Precipitation Measurement, which was held in St Moritz, Switzerland, from 4 to 7 December 1989 addressed these precipitation-measurement problems and broader ones concerning the interaction between climate and the global water cycle. The Workshop was jointly organized by the WMO, the International Association of Hydrological Sciences (IAHS) and the Swiss Federal Institute of Technology (ETH).

At present the 160 000 rain-gauges (about 4000 in the United Kingdom alone) distributed over the land area of the globe, along with weather radars (8 in the United Kingdom) and satellite observations go a long way towards providing adequate meteorological information about rainfall over populated regions. However, they do not yet provide the accurate values of precipitation falling at a particular place on the earth's surface or over specific river catchments.

Water is as essential to our existence as the very air we breathe. Without rain, snow and other forms of precipitation to water the soil, raise the rivers and recharge the reservoirs, the economy and society of the planet would soon stop. But man is also affected by too much rain — floods are among the most serious disasters. More accurate information on this phenomenon is needed by hydrologists and all those concerned with water availability in the face of a changing climate.

The can-type precipitation gauge, in common use, has certain inherent deficiencies. Because most countries have developed their own gauges, each with its own characteristics, comparisons of precipitation amount across international boundaries may be difficult. Accurate assessments of global precipitation are also very difficult because there are virtually no measurements made over the oceans. Such information must be inferred from ground-based radar and satellite observations, which themselves rely on conventional rain-gauge measurements for calibration.

The Workshop studied these problems by bringing together experts in determining precipitation by various means, to promote improvements and to hasten the move towards truly homogeneous measurements. It directed attention to the research needed, especially in the World Climate Programme and Global Energy and Water Cycle Experiment (GEWEX) which is being planned as the major international effort in the study of the climate for the latter half of the 1990s.

New Meteorological Office buildings at Bracknell

For some years it has been acknowledged that the amount of accommodation space available to staff at Bracknell has been inadequate. As a consequence, the use of new buildings giving increased space, has commenced.

Three new office blocks adjacent to the main Headquarters building have been acquired, and two of these are to be named the Johnson and Sutton Buildings after past Heads of the Office (see below). The Sutton Building is already occupied by the Commercial Section of the Office; the Johnson Building will soon be occupied by staff responsible for data provision and consultancy. The third building will house the staff who will be at the forefront of the United Kingdom's research into climate change and it is felt that the name 'Climate Research Centre' will be a sufficiently clear identification of this building and its purpose.

The use of a further building, to replace the premises currently used at Eastern Road to house the Archives, has also been negotiated. These new premises for the Archives will be known as the Scott Building.

The list of 'named' parts of the Office includes: the FitzRoy, Napier Shaw, Dines and Richardson Wings of the Main Building, the Experimental Site at Beaufort Park, Easthampstead, and the Simpson Building at Western Road, Bracknell (which houses the stores and test facilities).

Listed below are short notes about the meteorologists who are commemorated in this way. Those who were in charge of the Office are collectively referred to as 'Heads' — in reality the name of this position has changed several times.

Vice-Admiral R. FitzRoy, FRS, 1805–1865. Head 1855–65.

In his earlier days Fitzroy captained HMS *Beagle*, with Charles Darwin on board as naturalist, and at one stage was the Governor of New Zealand. While at the Board of Trade, which was responsible for Meteorological Services at that time, he introduced storm warnings and the issue of daily forecasts to the Press.

R.H. Scott, MA, FRS, 1833–1916. Head 1867–1900.

Scott was responsible for the setting-up of the first official weather observing stations in the United Kingdom, to provide data for forecasting and climate studies. He was also interested in the meteorology of the oceans. During the period 1874–1900 he was secretary to the International Meteorological Committee.

Sir William Napier Shaw, D.Sc, FRS, 1854–1945. Head 1900–20.

Shaw initiated the systematic study of atmospheric processes, which laid the foundations for scientific weather forecasting. He had a particular interest in upper-air studies, and was president of the International Meteorological Committee from 1907 to 1923.

Sir George Simpson, KCB, CBE, D.Sc, LL D, FRS, 1878–1965. Head 1920–38.

As a younger man, Simpson was a pioneer of Antarctic meteorology. He supervised the integration of the Meteorological Office into the Air Ministry in the early 1920s. After retirement he returned to the Office to take charge of the Observatories, where he specialized in studies of the electrical charging in thunderstorms.

Sir Nelson Johnson, KCB, D.Sc, ARCS, 1892–1954. Head 1938–53.

Johnson's early days were spent in studies of atmospheric diffusion and temperature variations close to the ground. Later, as head of the Office, he was responsible for the installation of stations for making upper-air soundings and sferics measurements. He was the last president of the International Meteorological Organization and the first of its replacement — the World Meteorological Organization.

Sir Graham Sutton, CBE, FRS, 1903–77. Head 1953–65.

Sutton was notable for promoting the exchange of ideas between the research and services sides of the Office, and the development of services to non-aviation customers. During his tenure, the Office acquired its first electronic computer.

W.H. Dines, FRS, 1855–1927.

After a 4-year apprenticeship in steam-locomotive design and building, and 3 years studying mathematics at Cambridge, Dines turned his attention to the measurement of meteorological variables. He designed a pressure-tube anemometer and a tilting-siphon rain-gauge, both of which are still in use to this day.

L.F. Richardson, D.Sc, FRS, 1881–1953.

Richardson's meteorological work showed a rare combination of theoretical and experimental ability. His studies of atmospheric turbulence are commemorated in the Richardson number. His pioneering work on numerical weather prediction was ahead of its time, there being neither adequate observations of the atmosphere nor computers available for his methods to be exploited.

Rear-Admiral Sir Francis Beaufort, FRS, 1774–1857.

Beaufort is mainly known for introducing two systems for describing aspects of weather which do not rely upon a knowledge of English. These are his Scale of Wind Force in which wind speeds are described by numbers, and a Notation of Weather using letters.

Books received

The listing of books under this heading does not preclude a review in the Meteorological Magazine at a later date.

Global climate change, by S.F. Singer (New York, Paragon House, 1989) divides the problems into inadvertent human intervention, purposeful human intervention and outside human intervention. The common themes relating to human survival are investigated.

Meteorology and World War II, Parts I and II, edited by B.D. Giles (Royal Meteorological Society, 1987, 1989) contain descriptions of the various meteorological endeavours of the period by many people who were there. The two volumes are the products of two conferences held at the University of Birmingham in 1986 and 1988.

Satellite and radar photographs — 25 March 1990 at 0900 and 1500 UTC

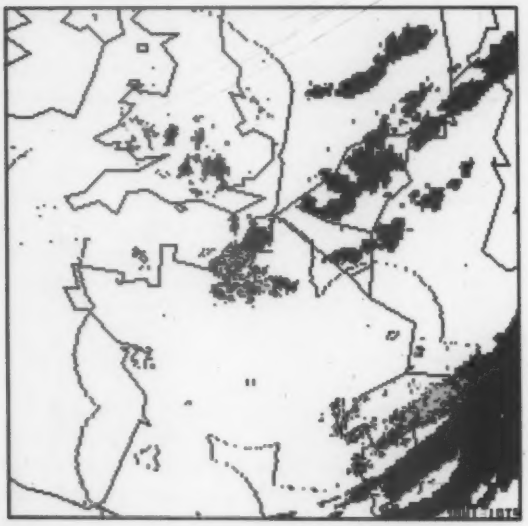

Figure 1. COST 73 (Co-operation in Science and Technology project 73) satellite and radar picture at 0900 UTC on 25 March 1990. Dark blue represents cloud tops colder than −15 °C. Green, yellow, red and light blue represent progressively increasing rainfall rates. Coastlines, national boundaries and the limits of radar coverage are shown in black.

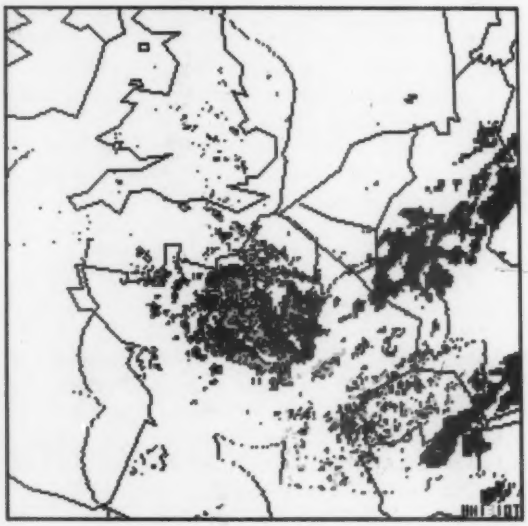

Figure 2. As Fig. 1 but for 1500 UTC on 25 March 1990.

The Meteosat satellite and radar photographs shown in Figs 1 and 2 illustrate the intensification of showers due to daytime heating in a cold northerly airstream. Cloud colder than −15 °C is shown (in dark blue) except at pixels where precipitation is also occurring, when the radar-derived rainfall intensity is shown. At the present time radar information is restricted to the British Isles, France and Switzerland.

At 0900 UTC (Fig. 1) the leading edge of the cold airmass was located over Switzerland, marked by a cold front and related band of cloud and precipitation. Within the cold air, cloud and showers were chiefly restricted to a trough extending from Denmark to southern Britain and northern France. Convection was enhanced by daytime heating, identified at 1500 UTC (Fig. 2) by a considerable increase in the area and intensity of showers. Synoptic observations indicated that hail and thunder occurred within some of the showers near the trough. Elsewhere showers were generally less heavy and over western France and western and northern Britain showers were either absent or very light due to the influence of a large area of high pressure (see Fig. 3).

G.A. Monk

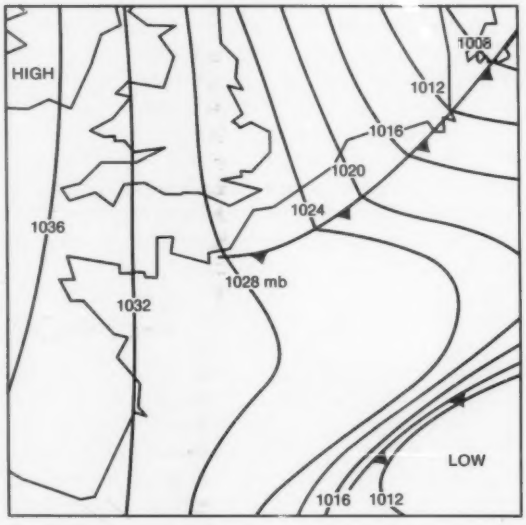

Figure 3. Surface analysis at 1200 UTC on 25 March 1990.

GUIDE TO AUTHORS

Content

Articles on all aspects of meteorology are welcomed, particularly those which describe results of research in applied meteorology or the development of practical forecasting techniques.

Preparation and submission of articles

Articles, which must be in English, should be typed, double-spaced with wide margins, on one side only of A4-size paper. Tables, references and figure captions should be typed separately. Spelling should conform to the preferred spelling in the *Concise Oxford Dictionary* (latest edition). Articles prepared on floppy disk (Compucorp or IBM-compatible) can be labour-saving, but only a print-out should be submitted in the first instance.

References should be made using the Harvard system (author/date) and full details should be given at the end of the text. If a document is unpublished, details must be given of the library where it may be seen. Documents which are not available to enquirers must not be referred to, except by 'personal communication'.

Tables should be numbered consecutively using roman numerals and provided with headings.

Mathematical notation should be written with extreme care. Particular care should be taken to differentiate between Greek letters and Roman letters for which they could be mistaken. Double subscripts and superscripts should be avoided, as they are difficult to typeset and read. Notation should be kept as simple as possible. Guidance is given in BS 1991: Part 1: 1976, and *Quantities, Units and Symbols* published by the Royal Society. SI units, or units approved by the World Meteorological Organization, should be used.

Articles for publication and all other communications for the Editor should be addressed to: The Chief Executive, Meteorological Office, London Road, Bracknell, Berkshire RG12 2SZ and marked 'For Meteorological Magazine'.

Illustrations

Diagrams must be drawn clearly, preferably in ink, and should not contain any unnecessary of irrelevant details. Explanatory text should not appear on the diagram itself but in the caption. Captions should be typed on a separate sheet of paper and should, as far as possible, explain the meanings of the diagrams without the reader having to refer to the text. The sequential numbering should correspond with the sequential referrals in the text.

Sharp monochrome photographs on glossy paper are preferred; colour prints are acceptable but the use of colour is at the Editor's discretion.

Copyright

Authors should identify the holder of the copyright for their work when they first submit contributions.

Free copies

Three free copies of the magazine (one for a book review) are provided for authors of articles published in it. Separate offprints for each article are not provided.

May 1990

Editor: B.R. May
Editorial Board: R.J. Allam, R. Kershaw, W.H. Moores, P.R.S. Salter

Vol. 119
No. 1414

Contents

Contributions: It is requested that all communications to the Editor and books for review be addressed to the Chief Executive, Meteorological Office, London Road, Bracknell, Berkshire RG12 2SZ, and marked 'For *Meteorological Magazine*'. Contributors are asked to comply with the guidelines given in the *Guide to authors* which appears on the inside back cover. The responsibility for facts and opinions expressed in the signed articles and letters published in *Meteorological Magazine* rests with their respective authors.

Subscriptions: Annual subscription £30.00 including postage; individual copies £2.70 including postage. Applications for postal subscriptions should be made to HMSO, PO Box 276, London SW8 5DT; subscription enquiries 071–873 8499.

Back numbers: Full-size reprints of Vols 1–75 (1866–1940) are available from Johnson Reprint Co. Ltd, 24–28 Oval Road, London NW1 7DX. Complete volumes of *Meteorological Magazine* commencing with volume 54 are available on microfilm from University Microfilms International, 18 Bedford Row, London WC1R 4EJ. Information on microfiche issues is available from Kraus Microfiche, Rte 100, Milwood, NY 10546, USA.

ISBN 0 11 728665 6

ISSN 0026–1149